Edinburgh Research Explorer

Leidenfrost droplets on microstructured surfaces

Leidenfrost droplets on microstructured surfaces

Gail Duursma[1*], Ross Kennedy[1], Khellil Sefiane[1,2], Yong Yu[3]

[1]School of Engineering, The University of Edinburgh, King's Buildings, Mayfield Road, Edinburgh EH9 3JL, United Kingdom

[2]International Institute for Carbon-Neutral Energy Research(I2CNER), Kyushu University, 744 Motooka, Nishi-ku, Fukuoka 819-0395, Japan

[3]School of Aerospace Engineering, Beijing Institute of Technology, 5 South Zhongguancun Street, Haidian District, Beijing 100084, People's Republic of China

[*]Address correspondence to Dr Gail Duursma, School of Engineering, The University of Edinburgh, The King's Buildings, Mayfield Road, Edinburgh EH9 3JL, UK

E-mail: gail.duursma@ed.ac.uk

Phone Number: 0 (+44) 131 650 4868, Fax Number: 0 (+44) 131 650 6551

ABSTRACT

The lifetime of a droplet deposited on a hot plate decreases when the temperature of the plate increases, but above the critical Leidenfrost temperature, the lifetime suddenly increases. This is due to the formation of a thin layer of vapour between the droplet and the substrate which plays a double role: first it thermally insulates the droplet from the plate and second it allows the droplet to "levitate." The Leidenfrost point is affected by the roughness or microstructure of the surface. In this work, a silicon surface with different micro-structured regions of square-pillars was prepared such that there is a sharp transition (boundary) between areas of different pillar spacing. The Leidenfrost point was identified in experiments using water droplets ranging in size from 8 - 24 microlitres and the behaviour of the droplets was recorded using high-speed digital photography. The Leidenfrost point was found to vary by up to 120 °C for pillar spacings from 10 - 100 microns. If the droplet is placed on the boundary between structured sections, the droplet becomes asymmetric and may move or spin. An axisymmetric CFD model is also presented which shows qualitative agreement with experimental observations.

.

INTRODUCTION

The interaction of droplets with hot surfaces is relevant to a wide range of applications. When surfaces are above a critical temperature the droplets are observed to levitate. This latterly-called Leidenfrost effect was first reported in 1732 by Boerhaave [1] who noted that ethanol droplets deposited on superheated metal surfaces did not boil rapidly as expected and indeed persisted longer than droplets on cooler surfaces. In 1756, Leidenfrost made similar observations about the lifetime and mobility of water droplets deposited on a hot silver spoon in his paper, 'De Aquae' and gave his name to the phenomenon. The Leidenfrost effect can hamper cooling technologies in high heat flux applications and it is crucial for safety to avoid dryout in nuclear reactors, the consequences of which are catastrophic [2]-[3]. Other applications exploiting the Leidenfrost phenomenon are printing, jet impingement and vitrification of biofluids by levitation above liquid nitrogen – in this latter application the inhibition of heat transfer is beneficial as it produces the right freezing rate for cell preservation.

Above the Leidenfrost Point (LFP), droplets begin to float on an insulating layer of their own vapour (see Fig. 1), resulting in a local maximum for droplet lifetime and a substantial increase in mobility, due to the large reduction in friction. The droplet levitation resulting from the Leidenfrost effect has been harnessed to direct droplet motion through mechanical macro-scale ratchets and has even been used to produce mazes [4]-[5].

In many industrial situations, operating in the Leidenfrost boiling regime is highly undesirable due to the inhibition to heat transfer. In metallurgical processes such as quenching and spray-cooling, the Leidenfrost effect inhibits the control of cooling by means of the insulating vapour layer. Fast cooling is necessary to maintain the mechanical strength of material, while uniform temperature profiles prevent deformation [6]-[7].

The Leidenfrost effect has implications in both high heat flux microelectronics cooling systems and in fire-fighting emergencies where it is necessary for rapid heat removal. Indeed, accident reports following the Fukushima nuclear disaster have cited the inverse Leidenfrost effect as a contributor to the inability to cool the fuel system effectively while following emergency procedures [8]-[9].

Being able to alter the LFP of systems to either avoid or deliberately enter the Leidenfrost boiling regime is of particular interest across a wide variety of industrial applications. Being able to raise the LFP, by as much as 100 °C, can vastly extend the temperature range where Leidenfrost does not need to be considered for both process design and safety. Many properties such as thermal diffusivity and pressure are also shown to affect the Leidenfrost point, as shown in Orejon *et al.* [10].

Surface roughness has always been understood as a key parameter: measurements of the LFP on two surfaces of the same material have been shown to vary greatly depending on whether the material was polished or rough. [11]-[20].

Altering the Leidenfrost point may also be done by exploiting hydrophobicity of surfaces and/or structuring them. Liu and Craig [12] examined hydrophobic smooth flat substrates and found that Leidenfrost levitation occurred at lower substrate temperatures. Vakarelski *et al.* [11] used combinations of chemical modification and surface heterogeneity to stabilise vapour layers surrounding spherical substrates and avoid nucleate boiling.

Recently, there has been particular interest in the influence of micro- and nano-structures being used to alter the LFP for enhanced boiling. Kwon *et al.* [16] carried out a systematic study of the effect of microstructures on the LFP of a water-silicon system over a range of micropillar parameters. The authors demonstrated experimentally that the Leidenfrost point could be shifted by as much as 100 °C by manipulating surface structure. They proposed a

mechanism to describe the variation of the LFP due to the presence of the microstructure array. They surmised that as the surface was highly wetting, there would be contact between the tops of the micropost array and the underside of the droplet, and that this contact would result in a force balance between the surface tension ($\Delta p_{cap} \sim \gamma/b$) acting downwards and a vapour pressure (which can be modelled as radial Poiseuille flow) acting upwards. The authors suggest that the Leidenfrost state exists if the ratio of these competing vertical forces balances is approximately unity; $\Delta p^{*}_{vap} / \Delta p_{cap} \sim 1$.

On the other hand, modelling and simulation of these complex phenomena is sparse and most studies have been limited to flat surfaces. For instance, Rueda Villegas [21] has performed numerical simulations of the Leidenfrost effect using the level set method for droplets falling onto a smooth substrate. Using a numerical approach they were able to capture some aspects of this behaviour.

Despite the numerous studies on the Leidenfrost phenomenon, recent findings on the significant effect of substrate roughness and structure demonstrate the need for further investigation of the phenomena. In the present study an experimental investigation of the effect of size and spacing of microstructures on Leidenfrost point is undertaken. Furthermore a numerical model is presented to describe the experimental observations.

EXPERIMENTAL APPARATUS and PROCEDURES

A silicon micro-structured surface was produced using deep etching. A 4 inch silicon wafer was treated with a photoresist polymer before standard lithography and etching techniques were used to impose the design, through a glass mask, onto the surface. The surface was post-processed with plasma oxidation to remove any residue from the etching process and to ensure that droplets deposited onto its surface are completely wetting (superhydrophilic). The microstructure design pattern imprinted onto the wafer is illustrated in Figure 2. All pillars

are square-topped; arranged in a grid-like array and have a uniform height of 10 μm, a height sufficient, it is felt, not to be a significant influence on wetting. The wafer (as shown in Figure 2) was divided into sections, each of which was created with a unique pillar thickness and spacing (detailed in Figure 3) to give a wide range of microstructures to examine. The surface was inspected visually using an optical microscope and then analysed in detail using a white light interferometer to ensure the integrity and accuracy of the micropillars design (see Figure 2 (b)).

The sizes and spacing of the various configurations is shown in Figure 3. The sections are directly adjacent to each other so that a boundary of structure is available for experimentation. In this work, experiments with 10 μm thickness pillars only is included; the effect of pillar thickness will be examined in future work.

The surface was heated using a thermostatically controlled hot plate and the Leidenfrost point was measured for each individual microstructured section. A high-speed camera was used to record Leidenfrost behaviour in detail, for droplets deposited both on single regions and on the interface between two regions of different structure. Droplets were carefully placed on the surface (i.e. the droplets had a Weber number of unity) and the LFP was measured for three separate droplet sizes: 15 μL, 8 μL and 24 μL, Figure 4.

RESULTS, ANALYSIS and DISCUSSION

A digital goniometer was used to measure equilibrium contact angles of water droplets on each structured surface on the wafer (see Figure 5) at ambient temperature. Droplets were deposited using an electronically controlled syringe to consistently produce droplets of 5 μL. Equilibrium contact angles for droplets measured using the goniometer are shown in Figure 5 (b) and were all indeed hydrophilic and of the range 6.18° – 23.90°.

The wafer was then placed on the thermostatically controlled hotplate and observations were made of deposited droplets of sizes 8, 15 and 24 microlitres. It is worth noting that the radii for these drops are 1.2, 1.5 and 1.8mm respectively. All these radii are below the capillary length which indicates that they would be spherical. The Leidenfrost temperature is identified as that at which complete levitation of droplets is observed. The experimental observations revealed abehaviour of deposited droplets in agreement with previously reported observations in the literature [22]. At low temperatures, droplets tend to wet the substrate, whereas above a threshold temperature, the droplets levitate on a vapour cushion. This observation was consistent for all investigated surfaces, Figure 6.

The threshold temperature at which droplets levitate depended on the design of the microstructures. This will be investigated in more detail further on. The size of droplet is also found to affect the LFP. In agreement with previous observations [22], larger droplets required higher temperatures to levitate, Figure 7. The data from Kwon *et al.* [16] are also reported on Figure 7 for the sake of comparison. For all droplets, the LFP was found to increase monotonically with the pillar spacing, Figure 7. This trend is in agreement with the reported observations of Kwon *et al.* [16], though their results, which used 30 microlitre droplets, were consistently lower than we would expect for a droplet size larger than our greatest size. Differences in surface thermal properties and other parameters may account for this discrepancy.

As can be seen in Figure 7, both microstructure and droplet size have a significant influence on the LFP on the silicon surface. The range of the LFP varies from 240°C for the 8 microlitre droplet with narrow pillar spacing to 410°C for the 24 microlitre droplet at widest pillar spacing. This is a far greater LFP variation than has previously been recorded in literature for silicon surfaces and an extension of the data reported by Kwon *et al.* [16].

Work by Biance *et al.* in 2003, previously also explored the effect of droplet size on the LFP [22]. They showed that droplet evaporation occurs almost entirely through the underside. Kruse *et al.* [17] explored the idea of possible distortions in the droplet underside due to the presence of microstructures, shown schematically in Fig 8(inset). This increases the available area for heat transfer and hence evaporation. Our experimental observations, as well as the above findings, led us to explore two mechanisms and their effect on heat transfer and evaporation. The first of these is the idea of additional area for heat transfer for droplets above microstructures. As the Leidenfrost state can be said to occur when the lift force created by the evaporating vapour overcomes the downward force of gravity, an increase in the available area for heat transfer to occur should reduce the temperature required to achieve levitation. The increased area of the underside of the droplets is, however, too complex to measure. Instead we use the increase in surface area due to the micropillars. This would be the maximum possible (upper bound) increase in surface area. This was nondimensionalised using the base area of a flat surface. Plotting the measured LFP against this dimensionless area (Figure 8) shows that in cases where the LFP is highest, the surface area approaches that of a flat surface (LFP ~320°C for the case of the smallest droplet), presumably as the distorted area decreases and hence a higher temperature is required to achieve the Leidenfrost state. This demonstrates the correlation between the Leidenfrost point and the distortion in surface area, which is a strong argument in favour of this mechanism.

The second mechanism investigated was the temperature distribution in the substrate. The heat transfer to the droplet may be predominantly from the tips of the micropillars, since these are closest to the droplet, such that the effective area available for heat transfer to occur is equivalent only to the area of the tops of the pillars themselves (Fig. 9(inset)) where the vapour film is thinnest, and the heat path distance is least. Plotting, in Fig 9, the LFP measured against this Effective Area for heat transfer (a ratio of the surface area of the tops

of the pillars to the area of a flat surface) shows a similar trend to Figure 8. Where there is more surface area available for heat transfer to occur, the LFP is lower. This also gives credibility to this mechanism. It however points to the fact that both mechanisms highlight the same relevant factor, namely the area for heat transfer.

Unlike Kwon *et al.*, the above analysis demonstrates that the relevant parameter in Leidenfrost levitation on microstructured surfaces is the effective heat transfer area. This opens the way for numerical simulation which incorporates heat transfer and evaporation.

NUMERICAL SIMULATIONS

A two-dimensional axisymmetric numerical model in cylindrical coordinateswas constructed akin to the pillared surface to allow for reasonable simulation times. The domain, initial and boundary conditions are shown in Figure 10. The initial conditions comprise a spherical droplet, of 8 microlitre size, having a 180° contact angle with respect to the surface. Simulation boundary conditions are the wall and ambient temperatures. The simulations were performed with the commercial software, FLUENT, using the VOF method.

This approach to simulating liquid and gas phases as well as interfaces is similar to that developed by Kunkelmann and Stephan [23], to which we refer the reader, and provide, for brevity, a summary of the key equations we used below. The simulation solves the mass, momentum and energy conservation equations (equations 1,2 and 4 resp.) in both phases with boundary conditions between. The mass conservation equation is written as:

$$\frac{1}{\rho_q}\left[\frac{\partial}{\partial t}\left(\alpha_q \rho_q\right) + \nabla \cdot \left(\alpha_q \rho_q \overrightarrow{v_q}\right)\right] = \Sigma_{p=1}^n\left(\dot{m}_{pq} - \dot{m}_{qp}\right) \qquad (1)$$

where $\dot{m}_{qp}$ is the mass transfer from phase q to phase p and $\dot{m}_{pq}$ is the mass transfer from phase p to phase q. The momentum equation is as follows;

$$\frac{\partial}{\partial t}(\rho\vec{v}) + \nabla \cdot (\rho\vec{v}\vec{v}) = -\nabla p + \nabla \cdot [\mu(\nabla\vec{v} + \nabla\vec{v}^T)] + \rho\vec{g} + \vec{F} \quad (2)$$

A single momentum equation is solved throughout the domain, and the resulting velocity field is attributed to the phases. The properties ρ and μ are determined by the presence of the component phases in each control volume. In a multiphase system such as this, the density in each cell is given by

$$\rho = \sum_{q=1}^{n} \alpha_q \rho_q \quad (3)$$

All other bulk properties, such as viscosity, are computed similarly. The energy equation is written as;

$$\frac{\partial}{\partial t}(\rho E) + \nabla \cdot (\vec{v}(\rho E + p)) = \nabla \cdot [k_{eff}\nabla T] + S_h \quad (4)$$

Energy, E, and temperature, T, as treated as mass-averaged variables in the VOF method:

$$E = \frac{\sum_{q=1}^{n} \alpha_q \rho_q E_q}{\sum_{q=1}^{n} \alpha_q \rho_q} \quad (5)$$

where E_q for each phase is based on the specific heat of that phase and the value of temperature.

The formulation of the bulk values of properties such as ρ and k_{eff} (effective thermal conductivity) is the same for both phases. The source term, S_h, contains contributions from radiation, as well as volumetric heat sources.

Since we are dealing with an interface undergoing phase change, a sub-model representing the phase change process is required. The task of this sub-model for phase change can be

subdivided into the calculation of the local rate of evaporation and the calculation of corresponding source terms for conservation equations.

To calculate the local evaporation rate, the approach developed by Hardt and Wondra [24] was used. In their method, the evaporation mass flux is calculated from the interface temperature and the interfacial heat resistance;

$$j_{int} = \frac{T_{int} - T_{sat}}{R_{int}} \tag{6}$$

The interfacial heat resistance R_{int} is a measure of the magnitude of deviation of the interfacial temperature from the saturation value for a certain evaporation rate:

$$R_{int} = \frac{2-f}{2f} \frac{T_{sat}^{3/2} \sqrt{2\pi R_{gas}}}{\rho_v \Delta h_v} \tag{7}$$

Herein, the accommodation coefficient f takes into account molecular effects such as reflection of liquid molecules emitted from the interface during evaporation. Marek and Straub [25] point out that there is a lot of uncertainty regarding this coefficient. "Typical" values in literature vary by more than two orders of magnitude. The most commonly used value in the literature is, however, unity, as is used here. Numerical experiments showed that a variation of the accommodation coefficient in a range between 0.5 and 1 does not affect the results [23] significantly. Another approach has been formulated to obtain the expression for predicting the rate of evaporation, which is based on the statistical rate theory (SRT) [26]. It gives the expression for the evaporation flux in terms of the material properties and the molecular properties (the quantum mechanical vibrational and rotational characteristics) of the evaporating substance. There are no fitting parameters in the SRT expression for the evaporation flux [27]-[29]. SRT predicts the rate of molecular transport across the interface between macroscopic phases in terms of material and molecular properties that can be determined independently of the rate process considered. The theory is based on the transition

probability concept of quantum mechanics, the Boltzmann definition of entropy, and the local-equilibrium concept of thermodynamics. It allows one to predict the interfacial molecular transport rate. One of the issues raised by the SRT approach to kinetics concerns the prediction of unidirectional molecular transport rates across interfaces. The SRT prediction is that a unidirectional rate depends on the conditions in both phases. By contrast, from classical kinetic theory (CKT) it is predicted that the unidirectional rate of liquid evaporation depends only on the conditions in the liquid phase. The SRT approach leads to an expression for the unidirectional evaporation rate that depends on the conditions in both the liquid and vapour phases. As a result, there are differences in the values of the predicted net rates obtained from SRT and those obtained from either CKT or absolute rate theory and the approach behind equation (7) is used as a representative prediction method for numerical evaluation.

 The evaporation mass flux which is transferred through the liquid-vapour interface must be incorporated into the conservation equations. This is done by the definition of volumetric source terms.

The phase change model was programmed by a user defined function prescribing mass transfer; FLUENT automatically adds the source contribution to the relevant momentum, energy and scalar equations.

The two-dimensional adaptable mesh which is used for the simulation is shown in Figure 11. A very high mesh resolution is required near the heater surface in order to capture correctly the vapour layer flows and microstructures. The smallest cell in the gap has a width and height of around 1.25 μm. The mesh consists of escalating size cells in the horizontal and

vertical direction in order to keep the total number of cells as low as possible, in order to minimise computing time.

In order to distinguish between levitating drops and wetting ones, simulations at different temperatures were performed. In Figure 12 (a) at 127°C the droplet was attached to the surface and is therefore considered as below the Leidenfrost point whereas in Fig 12 (b) at 300°C the droplet levitation has occurred and is therefore deemed in Leidenfrost. The above criterion for the occurrence of Leidenfrost is consistently used in all subsequent simulations.

In Figure 13 a sequence showing the evolution of a droplet from the initial state to Leidenfrost levitation at 300°C is presented. This indicates that levitation occurs in a matter of milliseconds.

Simulations representing all microstructure designs as investigated experimentally, were run to determins the Leidenfrost point. A comparison of the experimentally observed Leidenfrost temperatures and of the numerical simulations is shown in Figure 14, giving reasonable agreement. The numerical simulations needs significant refinement as the 3D Cartesian microstructure together with the spherical geometry of the droplet presents significant challenges for numerical simulations. Also, simulations for a long period of real time take much computational time, and these are improvements to the simulations which we are working towards.

CORRELATION

The purpose of this study is to ascertain and quantify the effect of the microstructures on shifting the Leidenfrost temperature. More importantly, being able to predict this effect would be beneficial. For this reason, we attempt a first crude correlation which reflects the dependence of Leidenfrost temperature on spacing of microstructure. This is given as:

$$T_L = C_1 T_{flat} + C_2 b \qquad (8)$$

The correlation is fitted to the data in Figure 7 to evaluate the constants for the three droplet sizes, as shown in Figure 15. Extrapolation of this correlation beyond the pillar spacings used is invalid as the behaviour for very large pillar spacings would indeed also tend to that of a flat plate. We also recognise that the constants depend not only on droplet size but also on parameters such as nature of material, thermal properties and pillar height.

OUTLOOKS

During this study, some droplets were placed on the interface between structured regions and qualitative observations were made. If a droplet is suspended on the interface between two regions of differing microstructure design, a strong motive force is observed as it appears to tug violently and rotate erratically. There appears to be some kind of underlying oscillations in the supporting vapour phase, brought about as a result of the varying microstructure, which causes a strong impetus for the droplet to move. Additionally, droplets occasionally migrated on the wafer. It was observed that droplets which initially start in an area where they are in the Leidenfrost boiling regime but are then allowed to move into regions where the LFP is higher, remain in Leidenfrost. A full investigation and explanation of these observations is beyond the scope of this work.

CONCLUSIONS

We investigated experimentally the effect of the design of microstructures in the form of arrays of micropillars on the Leidenfrost phenomenon.

- The data demonstrate that increasing the spacing between the micropillars increases the Leidenfrost point, which is in agreement with literature.

- We proposed a new mechanism by which the micropillars affect the Leidenfrost point. This is based on modified surface area for heat transfer and evaporation.

- We developed a simplified numerical model which simulates the above conditions and the results show satisfactory agreement with the experimental data.

Future work includes the further recording, by means of the high-speed camera, of the behaviour of Leidenfrost droplets – how droplet lifetimes are affected by microstructure below the LFP and also the interactions that occur when a droplet is placed on a boundary between two differently structured regions.This will be obtained and analysed quantitatively through computational techniques. Furthermore, the effect of pillar thickness is also be investigated.

Acknowledgements

NOMENCLATURE

a   pillar thickness or width

A area

b pillar spacing

C constant

d diameter

E total energy

f accommodation coefficient

$\vec{F}$ force vector

$\vec{g}$ gravitational acceleration

h pillar height

Δh_v latent heat

j mass flux

k_{eff} effective thermal conductivity

$\dot{m}$ transfer mass flow rate

p pressure,

R heat resistance, gas-law constant

S_h source term

t time

T transpose of matrix, temperature

$\vec{v}$ velocity vector

Greek Symbols

α volume fraction

γ surface tension

μ dynamic viscosity

ρ density

Subscripts

cap   capillary

eff   effective

int   interface

p,q   phase designators

ref   reference

sat   saturation

vap   vapour

REFERENCES

[1] Lindeboom, G.A., *Herman Boerhaave: the man and his work*, Methuen, London, 1968.

[2] Leidenfrost, J.G., *De Aquae Communis Nonnullis Qualitatibus Tractatus*, Ovenius, Duisburg, 1756.

[3] Curzon, F.L., *The Leidenfrost phenomenon*, American Journal of Physics, vol 46 (8), 1978.

 [4] Lagabeau, G., Merrer, M., Clanet, C., and Quéré, D., *Leidenfrost on a ratchet*, Nature Physics, vol. 7, pp. 295-398, 2011.

[5] Grounds, A., Still, R., and Takashima,K., *Enhanced droplet control by transition boiling*, Scientific Reports, vol. 2, no. 720, pp. 1-5, 2012.

[6] Bernardin, J. D. and Mudawar, I., *, Film Boiling Heat transfer of Droplet Streams and Sprays*, International Journal of Heat and Mass Transfer, vol. 40, pp. 2579-2593, 1997.

[7] Lubben, T., Frerichs, F., Hoffmann, F., and Zoch, H.W., Rewetting behavior during immersion quenching, *New challenges in heat treatment and surface engineering-Conference in honour of Prof. Bozidar Liscic*, Dubrovnik-Cavtat, Croatia, 9-12 June 2009.

[8] Mochizuki, M., Singh, R., Nguyen, T., Nguyen, T., Mashiko, K., Saito, Y., and Wuttijumnong, V., *Completely passive heat pipe based emergency core cooling system for nuclear power reactor*, 16th International Heat Pipe Conference, Lyon, France, 20-24 May 2012.

[9] Buongiorno, J., Ballinger, R., Driscoll, M., Forget, B., Forsberg, C., Golay, M., Kazimi, M., Todreas, N., and Yanch, J., *Technical lessons learned from the Fukushima-Daichii accident and possible corrective actions for the nuclear industry: an initial evaluation*, MIT Center for Advanced Nuclear Energy Systems, Cambridge, MA, 2011.

[10] Orejon, D, Sefiane, K., and Takata, Y., *Effect of ambient pressure on Leidenfrost temperature*, Physical Review E, vol. 90, no. 5, pp. 053012-1 – 053012-6, 2014.

[11] Vakarelski, I.U., Patankar, N.A., Marston, J.O., Chan, D.Y.C., and Thoroddsen, S.T., *Stabilization of Leidenfrost vapour layer by textured superhydrophobic surfaces*, Nature, vol. 489, pp. 274-277, 2012.

[12] Liu, G., and Craig, V., *Macroscopically flat and smooth superhydrophobic surfaces: heating induced transition up to the Leidenfrost temperature*, Faraday Discussions, vol. 146, pp. 141-151, 2010.

[13] Bernardin, J.D., and Mudawar, I., *Transition boiling heat transfer of droplet streams and sprays*, Journal of Heat Transfer, vol. 129, no. 11, pp. 1605-1610, 2007.

[14] Quéré, D., *Leidenfrost dynamics*, Annual Review of Fluid Mechanics, vol. 45, pp. 197-215, 2013.

[15] Bernardin, J.D., and Mudawar, I., *The Leidenfrost point: experimental study and assessment of existing models*, Transactions of the ASME, vol. 121, no. 4, pp. 894-903, 1999.

[16] Kwon, H., Bird, J.C., and Varanasi, K.K., *Increasing Leidenfrost point using micro-nano hierarchical surface structures*, Applied Physics Letters, vol. 103, pp. 201601-1 – 201601-5, 2013.

[17] Kruse, C., Anderson, T., Wilson, C., Zuhlke, C., Alexander, D., Gogos, G., and Ndao, S.,*Extraordinary shifts of the Leidenfrost temperature from multiscale micro/nano structured surface*, Langmuir, vol. 29, no. 31, pp. 9798-9806, 2013.

[18] Agapov, R.A., Boreyko, J.B., Briggs, D.P., Srijanto, B.R., Retterer, S.T., Collier, C.P., and Lavrik, N.V., *Asymmetric wettability of nanostructures directs Leidenfrost droplets*, ACS Nano, vol. 8, no. 1, pp. 860-867, 2014.

[19] Cerro, D.A., Marín, A.G., Romer, G.R.B.E., Pathiraj, B., Lohse, D., and Huis, A.J., *Leidenfrost point reduction on micropatterned metallic surfaces*, Langmuir, vol. 28, no. 42, pp. 15106-15110, 2012.

[20] Ahn, H.S., Sathyamurthi, V., and Banerjee, D., *Pool boiling experiments on a nano-structured surface*, IEEE Transactions on Components and Packing Technologies, vol. 32, pp. 156-165, 2009.

[21] Rueda Villegas, L., *Simulation Numerique Directe de l'effet Leidenfrost*, PhD thesis, University of Toulouse, France, 2013.

[22] Biance, A.L., Clanet, C., and Quéré, D., *Leidenfrost drops*, Physics of Fluids, vol. 15, no. 6, pp. 1632-1637, 2003.

[23] Kunkelmann, C., and Stephan, P., *CFD simulation of boiling flows using the volume-of-fluid method within OpenFOAM.* Numerical Heat Transfer, Part A, vol. 56, pp. 631-646, 2009.

[24] Hardt, S., and Wondra, F., *Evaporation model for interfacial flows based on a continuum-field representation of the source terms,* Journal of Computational Physics, vol. 227, pp. 5871-5895, 2008.

[25] Marek R., and Straub, J., *Analysis of the evaporation coefficient and the condensation coefficient of water*, International Journal of Heat and Mass Transfer, vol. 44, pp. 39-53, 2001.

[26] Ward, C.A., Tucker, A.S., and So, C.W., *A Bubble Evolution Method for Diffusion Coefficient Measurements Utilizing the Critical Size Concept,* Journal of Physical Chemistry, vol. 83, pp. 543-550, 1979.

[27] Ward, C.A. and Sasges, M.R., *Effect of gravity on contact angle: A theoretical investigation*, Journal of Chemical Physics, vol. 109, pp. 3651-3660, 1998.

[28] Elliott, J.A.W. and Ward, C.A., *Temperature programmed desorption: A statistical rate theory approach*, Journal of Chemical Physics, vol. 106, pp. 5677-5684, 1997.

[29] Fang, G. and Ward, C.A., *Examination of the statistical rate theory expression for liquid evaporation rates*, Physical Review E, vol. 59, pp. 441-453, 1999.

Figure 15 Fitting Leidenfrost correlation to experimental data (colour online).

Figure 1 Nucleate to Leidenfrost boiling: (top) schematic; (bottom) photographic (adapted from Kwon

et al. [16])

(a)   (b)

Figure 2 Structure of the surfaces (a) schematic and (b) interferometer image (colour online)

	5, 10	10, 10	10, 20	5, 20	
	10, 80	10, 60	10, 50	10, 60	
5, 10	10, 70	10, 20	10, 90	10, 30	5, 10
5, 40	10, 40	10, 100	10, 10	10, 60	5, 5
5, 5	10, 60	10, 10	10, 100	10, 40	5, 40
5, 20	10, 30	10, 90	10, 20	10, 70	5, 20
	10, 70	10, 50	10, 60	10, 50	
	5, 40	10, 40	10, 30	5, 5	

Figure 3 Pillar width (first entry) and spacing(second entry) for each structured section of the

substrate
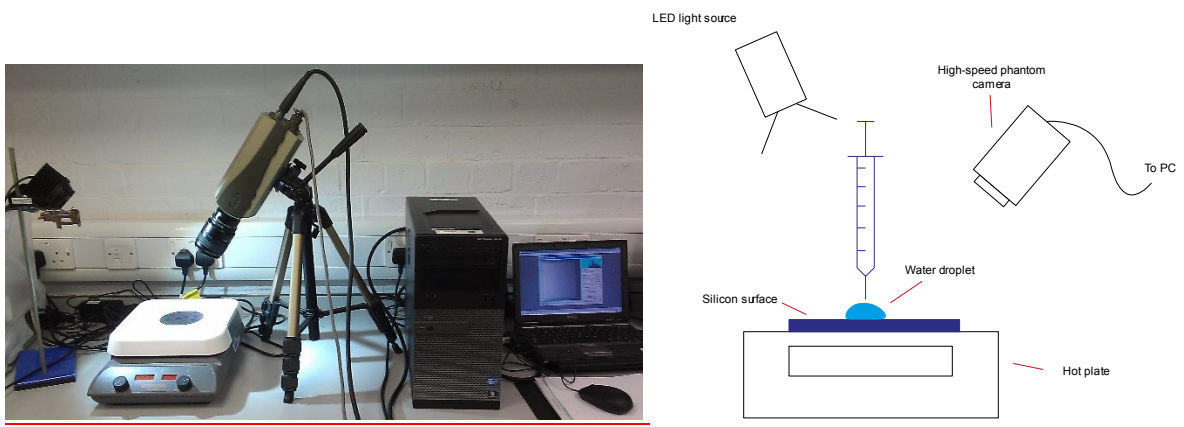
Figure 4 Schematic of apparatus (colour online)
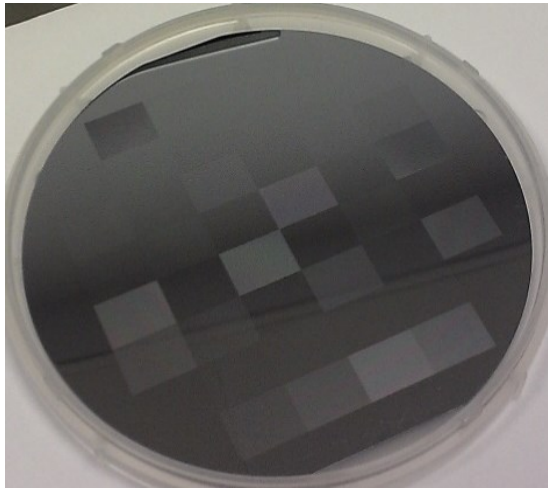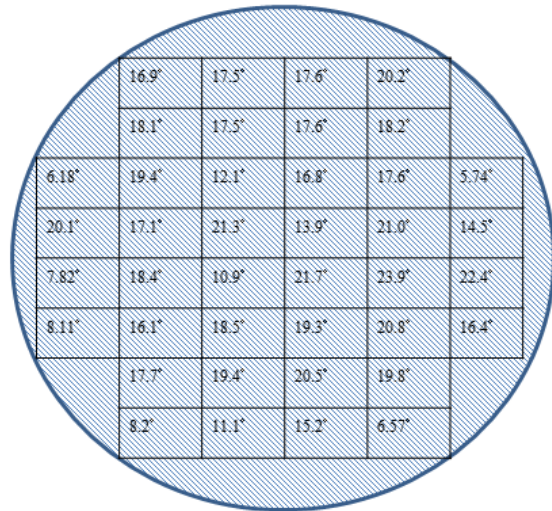
(a)   **(b)**

Figure 5 Wafer photograph (a) and (b) equilibrium contact angle results
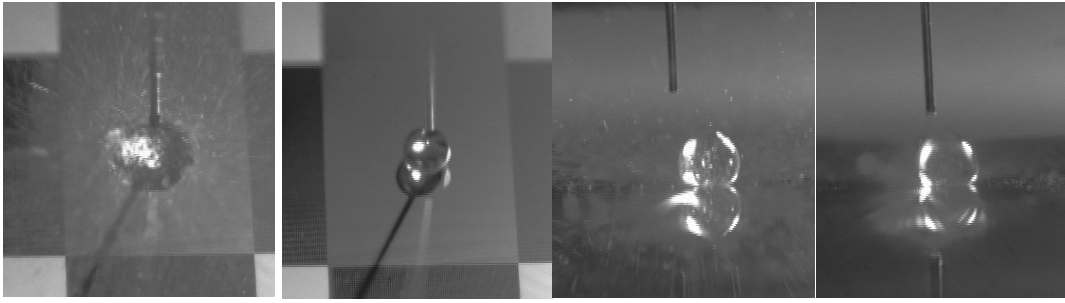
Figure 6 Photographs illustrating nucleate (<285°C) and Leidenfrost (285°C) boiling droplets
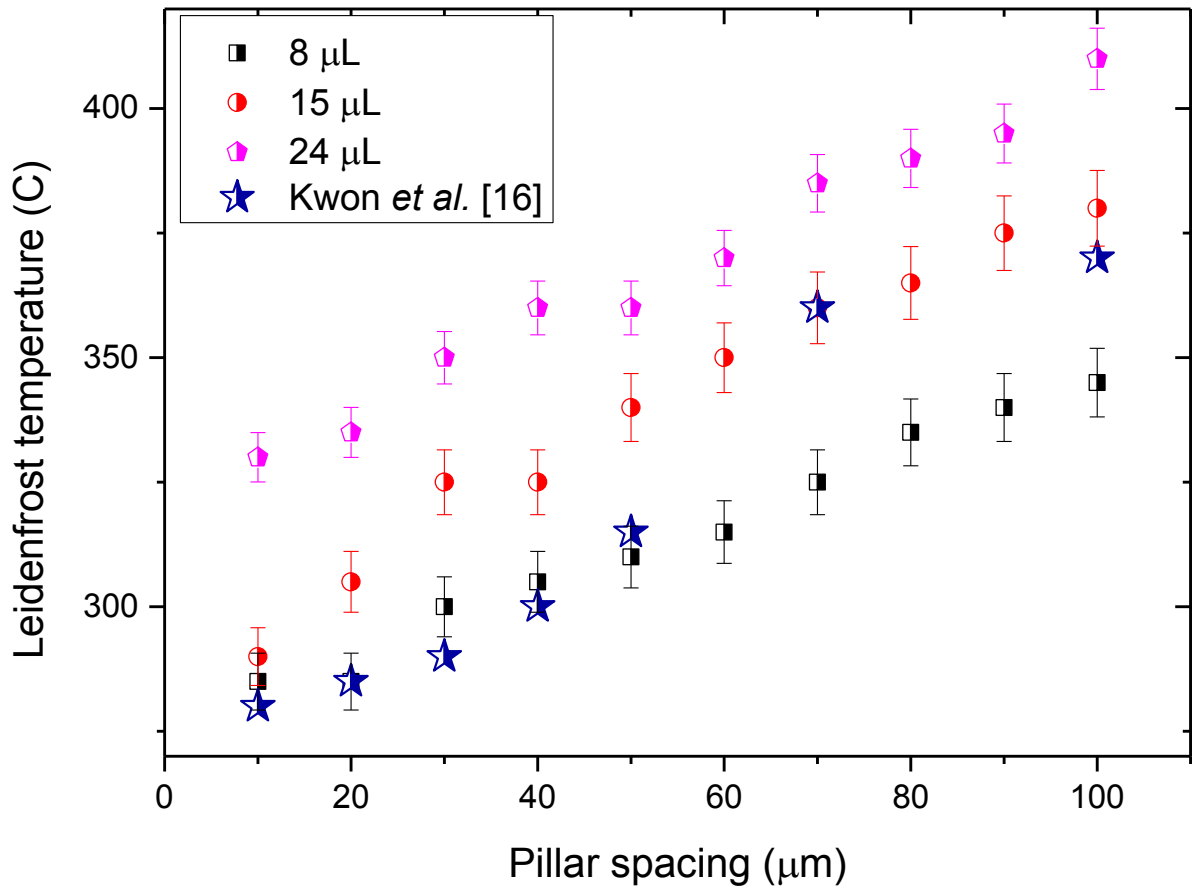
Figure 7 Graph of Leidenfrost temperature vs pillar spacing for 10 µm pillar thickness. Note that spherical droplet diameters are 2.4, 3.0 and 3.6 mm resp for the 8, 15 and 24 µL droplets resp. (colour online).
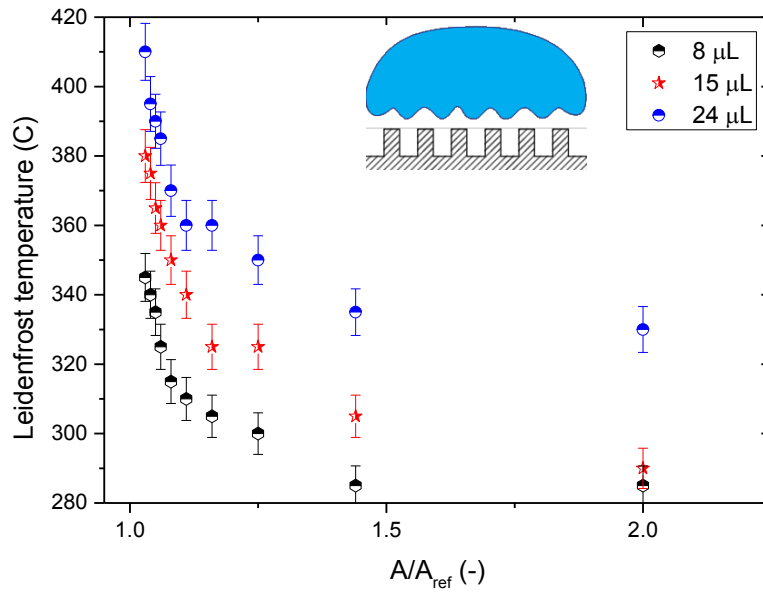
Figure 8 Graph of Leidenfrost temperature vs dimensionless area for 10 µm pillar thicknesses but variable spacing; inset: sketch of droplet deformation (colour online).
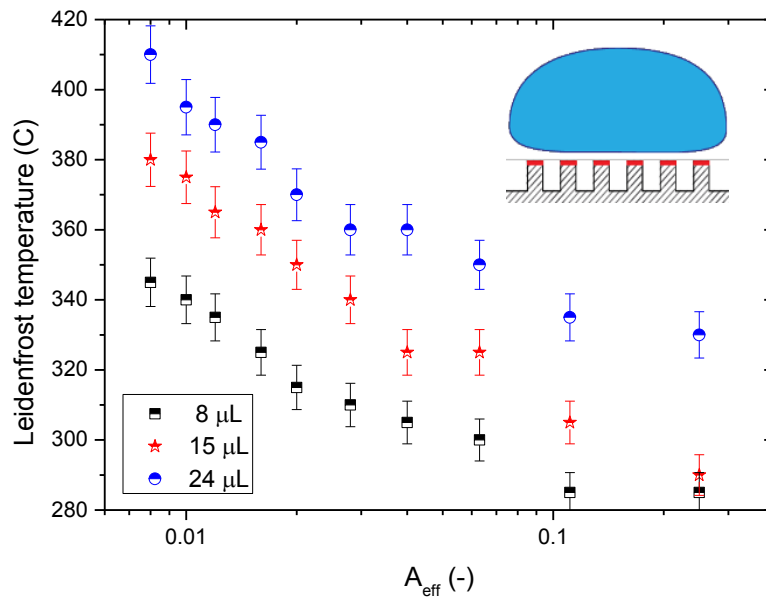
Figure 9–Graph of Leidenfrost temperature vs effective area, inset: effective area for heat transfer is reduced to the tops of the pillars (colour online).
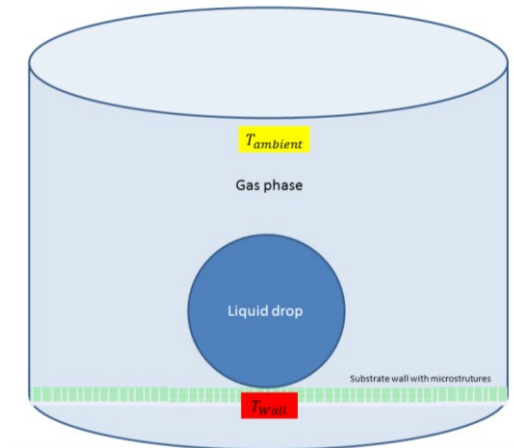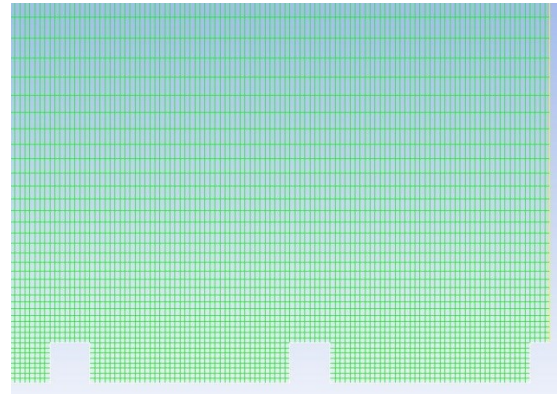
Figure 10 Numerical simulation schematic showing geometry and initial conditions, in cylindrical coordinates (colour online).
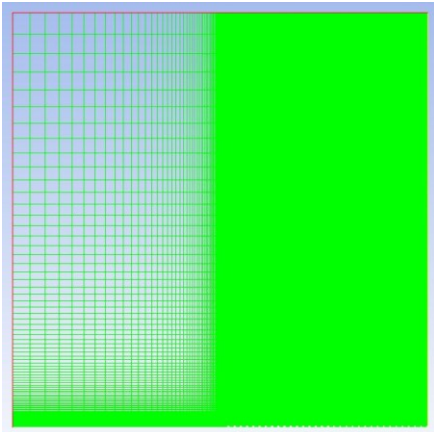
| Mesh of domain | zoom in near the gap |

Figure 11 Mesh used for numerical simulations; with radial direction horizontal and x-direction vertical; the origin is bottom right. Actual size of mesh is 4mm by 4mm. with the zoomed view being 110 µm by 80 µm (colour online).
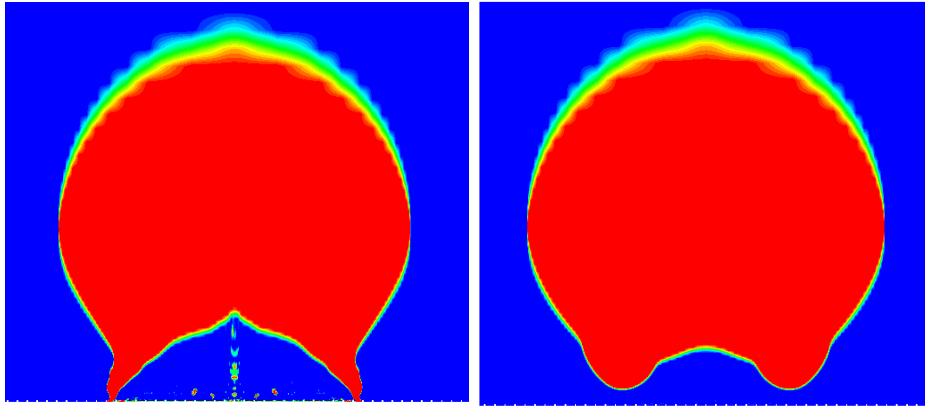
Figure 12 (Colour online) Contours of volume fraction of liquid (blue surround) and vapour (red centre): (a) T=127 °C , below the Leidenfrost Temperature; it can be seen that some very small droplets remain; (b) T=300 °C , Leidenfrost levitation achieved: the droplet floats upon a vapour cushion. All figures are of 2.5 mm by 2.5 mm actual size.
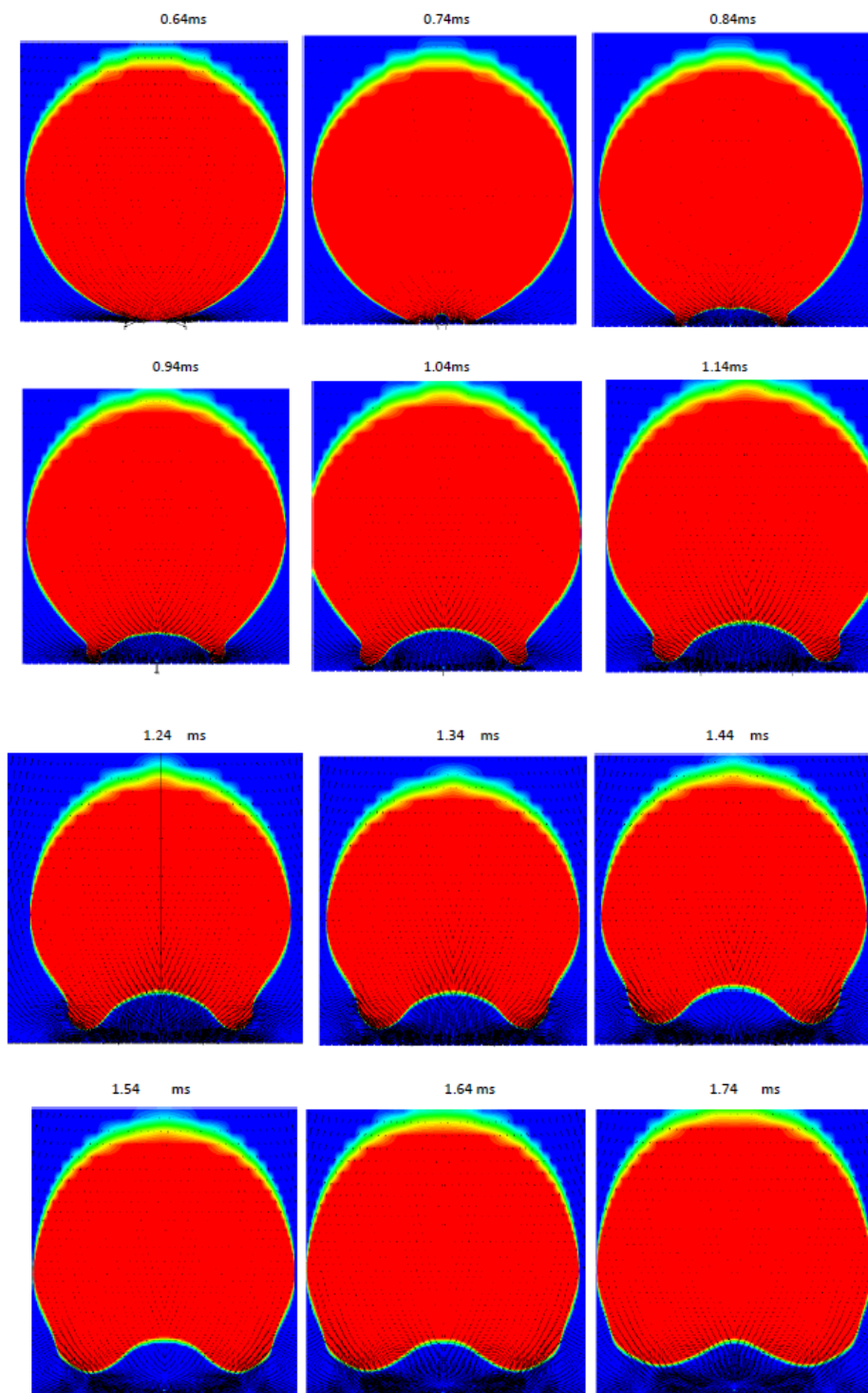
Figure 13 (colour online) Evolution of Leidenfrost levitation shown by presentation of volume fraction of liquid (blue surround) and vapour (red centre) at different times; T=300 °C . Velocity vectors are highlighted in both phases. All figures are of 2.5 mm by 2.5 mm actual size.
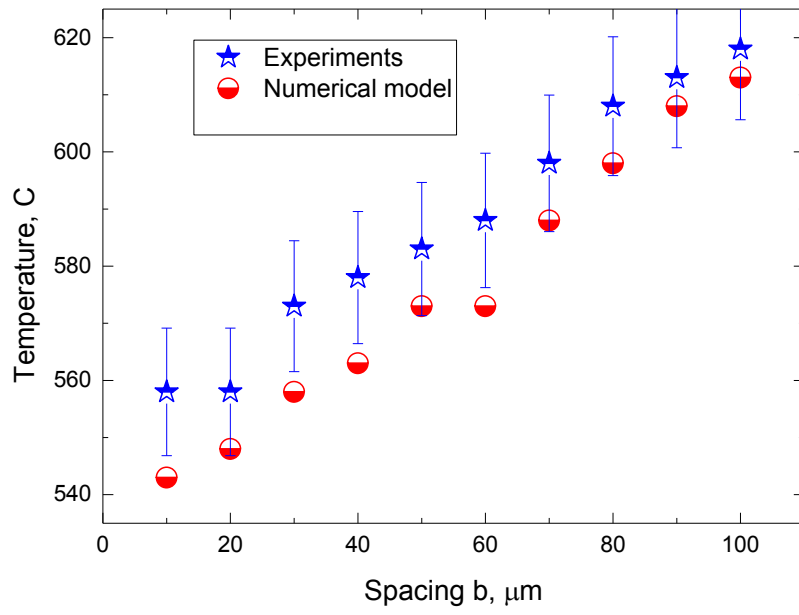
Figure14 Comparison of experimental Leidenfrost point and numerical simulation (colour online)
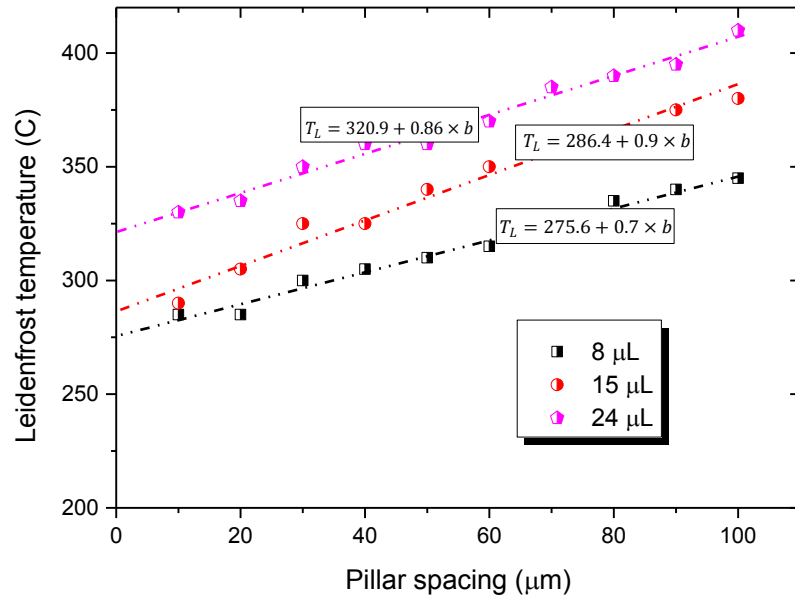
Figure 15 Fitting Leidenfrost correlation to experimental data (colour online).

Biographical details

Gail Duursma obtained her first degree in Chemical Engineering from University of Cape Town and her D.Phil from University of Oxford and is currently a Lecturer in Chemical Engineering at the University of Edinburgh.

Ross Kennedy was an undergraduate student at the University of Edinburgh from 2009 to 2014. He graduated with an MEng (Hons) degree in Chemical Engineering in 2014.

Khellil Sefiane has MSc and PhD degrees in Chemical Engineering. He is presently Professor and ExxonMobil Fellow at the University of Edinburgh and is Head of the Institute of Materials and Processes

Yong Yu obtained his PhD degree from Tsinghua University. He is Associate Professor with Beijing Institute of Technology and currently is a visiting scholar in the Institute of Materials and Processes at the University of Edinburgh.